GSI

GSI-Preprint-99-41
November 1999

PRODUCTION OF VERY NEUTRON-DEFICIENT ISOTOPES NEAR ^{100}Sn VIA REACTIONS INVOLVING LIGHT-PARTICLE AND CLUSTER EMISSION

M. La Commara, J. Gomez del Campo, A. D'Onofrio, A. Gadea, M. Glogowski, P. Jarillo-Herrero, N. Belcari, R. Borcea, G. de Angelis, C. Fahlander, M. Gorska, H. Grawe, M. Hellström, R. Kirchner, M. Rejmund, V. Roca, E. Roeckl, M. Romano, K. Rykaczewski, K. Schmidt, F. Terrasi

Gesellschaft für Schwerionenforschung mbH
Planckstraße 1 • D-64291 Darmstadt • Germany
Postfach 11 05 52 • D-64220 Darmstadt • Germany

Production of very neutron-deficient isotopes near ^{100}Sn via reactions involving light-particle and cluster emission

M. La Commara [a], J. Gómez del Campo [b], A. D'Onofrio [c,d], A. Gadea [e], M. Glogowski [f], P. Jarillo-Herrero [g], N. Belcari [h], R. Borcea [a], G. de Angelis [h], C. Fahlander [i], M. Górska [a], H. Grawe [a], M. Hellström [i], R. Kirchner [a], M. Rejmund [j], V. Roca [k,d], E. Roeckl [a], M. Romano [k,d], K. Rykaczewski [b,f], K. Schmidt [a], F. Terrasi [c,d]

[a] *Gesellschaft für Schwerionenforschung D-64291 Darmstadt, Germany*

[b] *Physics Division, Oak Ridge National Laboratory Oak Ridge, Tennessee 37831, USA*

[c] *Dipartimento di Scienze Ambientali, Seconda Università di Napoli I-81100 Caserta, Italy*

[d] *INFN, Sezione di Napoli Complesso Universitario di Monte S. Angelo, I-80126 Napoli, Italy*

[e] *Instituto de Física Corpuscolar, CSIC Valencia E-46100 Valencia, Spain*

[f] *Institute of Experimental Physics, Warsaw University PL-00681 Warszawa, Poland*

[g] *Universidad de Valencia E-46100 Burjassot (Valencia), Spain*

[h] *INFN, Laboratori Nazionali di Legnaro I-35020 Legnaro (Padova), Italy*

[i] *Division of Cosmic and Subatomic Physics, Lund University S-22100 Lund, Sweden*

[j] *CSNSM Orsay F-91405 Orsay Campus, France*

[k] *Dipartimento di Scienze Fisiche, Università di Napoli "Federico II" Complesso Universitario di Monte S. Angelo, I-80126 Napoli, Italy*

Preprint submitted to Elsevier Preprint *1 October 1999*

Abstract

The production of very neutron-deficient isotopes near ^{100}Sn has been investigated by using on-line mass separation of evaporation residues produced by heavy-ion induced complete-fusion reactions. We measured the cross sections for ^{99}Cd, ^{100}In, ^{101}Sn and ^{102}In via ^{58}Ni+^{58}Ni fusion reactions followed by cluster emission, and via ^{58}Ni+^{50}Cr fusion reactions accompanied by evaporation of protons, neutrons or α particles. Both types of reactions yield similar cross sections for the production of exotic nuclei near ^{100}Sn. The data are discussed in comparison with results obtained from statistical-model calculations.

PACS codes: 25.70.-z; 23.70.+j; 25.70.Jj; 27.60.+j

Key words: ^{100}Sn; production cross-sections; cluster emission; isotope separation on-line; β–delayed radiations

1 Introduction

Intense experimental and theoretical research has been lately devoted to the study of exotic nuclei far from the valley of β stability, which represents one of the central topics of present-day nuclear structure physics. In particular, the region around the doubly magic nucleus ^{100}Sn is a unique testing ground for investigating the structure of the atomic nucleus. Among the $N \cong Z$ nuclei, ^{100}Sn and neighbouring nuclei play a rather special role due to the appearance of several interesting phenomena: (*i*) the isospin symmetry is strictly connected to the question of proton-neutron pairing and isospin mixing; (*ii*) nuclei in this region lie near the proton drip-line, so far not yet fully explored; (*iii*) besides the known islands of α and proton radioactivity beyond ^{100}Sn, even the spontaneous emission of intermediate-mass fragments, that are particles with $Z \geq 3$ which we refer to as "clusters", might occur from ground states of nuclei in this area of the nuclide chart; (*iv*) the double shell closure at N=Z=50 involves features related to the astrophysical rp-process (1) which is expected to end near ^{100}Sn. Moreover, investigation on such nuclei offers the possibility to determine production cross-sections (σ), which is of great interest for testing and improving statistical-evaporation models. Recent in-beam experiments have shown that ^{58}Ni+^{58}Ni reactions with beam energies above 5·A MeV yield high σ values for nuclei below, although not very close, to ^{100}Sn. In this work (2), the residual nuclei were studied by their characteristic γ–rays emitted from excited states after the emission of clusters; the reaction products, ranging from ^{95}Ru to ^{100}Ag, lie rather close to the line of β stability, the corresponding production cross-sections being above 5 mb. The underlying mechanism was assumed to be complete fusion to the compound nucleus ^{116}Ba, followed by ^{12}C emission and light-particle evaporation. In this way it is possible to produce nuclei in states of angular momentum and excitation energy that are normally not populated via emission of light particles, such as protons, neutrons and α.

We investigated the production cross-sections of nuclei near ^{100}Sn by using heavy-ion induced fusion-evaporation reactions, and extended these studies in particular to those followed by cluster emission. In order to reach smaller σ values than those previously investigated (3) and to thus investigate the production of nuclei closer to ^{100}Sn, a more sensitive technique than an in-beam measurement is clearly necessary. The latter requirement was fulfilled by using the isotope separation on-line technique, which, as has been shown for ^{101}Sn (3), is very sensitive, i. e. is able to reach cross sections down to $\sim$10 nb. The experimental σ values were determined for the very neutron-deficient isotopes ^{99}Cd, ^{100}In, ^{101}Sn and ^{102}In, produced as evaporation residues after the following heavy-ion induced complete-fusion reactions: (*i*) ^{58}Ni+^{50}Cr, at 320 and 380 MeV incident energy, followed by evaporation of protons, neutrons and α particles from excited states of the compound nucleus ^{108}Te; (*ii*) ^{58}Ni+^{58}Ni, at incident energies ranging from 380 to 430 MeV, followed

by emission of clusters from excited states of the compound nucleus ^{116}Ba. The reactions ^{58}Ni+^{50}Cr and ^{58}Ni+^{58}Ni have been chosen in order to have a direct comparison between the cross sections of the light-particle evaporation mechanism and those of cluster-accompanied reactions for producing exotic nuclei near ^{100}Sn.

2 Experimental techniques

The experiment was performed at the mass separator on-line to the heavy-ion accelerator UNILAC of GSI (4). The experimental set-up is schematically shown in Fig. 1. A 30-40 particle-nA ^{58}Ni-beam impinged on a highly enriched target of either ^{50}Cr (3.6 mg/cm^2, 96.2%) or ^{58}Ni (3.8 mg/cm^2, 99.8%), respectively. After passing through thin heat shields and the entrance window, the recoiling reaction products were stopped in the hot graphite catcher (~2400 °K) inside a FEBIAD-E ion source (5). Subsequently they were released via solid-state diffusion and surface desorption, re-ionized to the 1^+ charge state, accelerated to 55 keV, and separated unambiguously according to their atomic mass A in a sector magnet. Two beamlines were simultaneously used, one to investigate the isotopes with A=99, 100 and 101 in sequencing measurements, and the other one to study ^{102}In. The A=99, 100 and 101 beams were alternatively implanted into two thin carbon foils mounted each in front of a ΔE-E silicon telescope which served for the measurement of β–delayed protons (βp). The technique of flipping the beam between two silicon telescopes was used in order to get halflife information without loosing counting statistics. The A=102 beam was implanted into a movable tape and then transported to a counting position which contained a ΔE-E silicon telescope and a HP-Ge detector for the measurement of both βp and β–delayed γ–rays ($\beta\gamma$). The counting times ranged from 4 hours for ^{99}Cd produced in the ^{58}Ni+^{50}Cr reaction, to 24 hours for ^{101}Sn produced in the ^{58}Ni+^{58}Ni reaction.

The experimental cross-sections for individual isotopes were deduced from mass-separated beam intensities, which were determined on the basis of the experimental βp and $\beta\gamma$ activities. Due to the more pronounced kinetic-energy and angular spreading of the residues after cluster emission, the σ values for the ^{58}Ni+^{58}Ni reaction had to be corrected for losses occurring in the collection of the recoils in the catcher mounted inside the ion source. This correction was performed by using a Monte Carlo simulation which takes into account both the energy and angular spread of the recoils due to their passage through target, heat shields and entrance window, and assumes a gaussian-shaped ^{58}Ni-beam profile with a halfwidth corresponding to the 8mm-diameter collimator in front of the target. This diameter was chosen as a compromise between the geometrical demands of the catcher-ion source system and the power density deposited in the target. For instance, for ^{99}Cd the recoil losses

amount to about 60% for a ^{58}Ni-beam with 375 MeV incident energy. The total separation efficiency, including release and ionization efficiency of the ion source as well as the transmission of the mass separator, is (15±3)% for ^{101}Sn (3), and was estimated to be the same (with a 50% relative-uncertainty) for ^{99}Cd, ^{100}In and ^{102}In. The βp and $\beta\gamma$ branching ratios were taken from previous experiments in the case of ^{99}Cd (7) and ^{102}In (6), whereas we used an experimental lower limit for ^{100}In (6) and a theoretical prediction for ^{101}Sn (3).

3 Experimental results

The experimental cross-sections from this work and from the literature are compiled in Table 1. For ^{99}Cd and ^{101}Sn produced in the ^{58}Ni+^{50}Cr reaction, the new data agree with those obtained previously (8) (3). For ^{102}In, ^{99}Cd and ^{101}Sn the ^{58}Ni+^{58}Ni reaction yields about the same σ values as those measured for the ^{58}Ni+^{50}Cr reaction. The dependence of σ upon the projectile energy is displayed in Fig. 2. In the ^{58}Ni+^{58}Ni reaction, the residual nuclei of interest could be in principle also be produced by light-particle emission. However, ^{58}Ni-beam energies are too low for this type of reaction, as can be seen from a comparison with results from statistical-model calculations (see next section). We thus infer the emission of ^{12}C clusters without detecting them.

4 Comparison with statistical model calculations

The experimental cross-sections can be compared to statistical-model predictions obtained by using the code BUSCO (9). It is based on the Hauser-Feschbach formula extended to as many as 400 evaporation channels, and takes into account the emission of light particles ($Z \leq 2$) as well as clusters ($Z \geq 3$) up to ^{40}Ca. In the calculation, a given channel, determined by Z, A and by the excitation energy of the emitted cluster, contains both discrete and continuum states. Moreover, we have calculated the σ values by means of the evaporation code HIVAP (10), which considers only the emission of light particles up to ^{4}He. The corresponding results are shown together with the experimental data in Fig. 2. For ^{102}In the data from the ^{58}Ni+^{58}Ni reaction are in very good agreement with the BUSCO predictions, whereas HIVAP predicts lower σ. This is a clear indication that indeed the emission of a ^{12}C cluster (plus one neutron and one proton) from the compound nucleus ^{116}Ba is the most likely process for ^{58}Ni energies between 280 and 400 MeV, the probability for emitting 3 α particles being at least one order of magnitude smaller. For ^{99}Cd a discrepancy occurs between the experimental data and the

BUSCO predictions. The HIVAP calculations overestimate the experimental ^{99}Cd results, indicating an onset of lack of reliability already at this distance from the β–stability valley. For ^{100}In the agreement between experimental data and BUSCO calculations is clearly getting worse: the code overestimates the cluster emission by about one order of magnitude. The HIVAP predictions underestimate the ^{100}In data, although there might be a sign of agreement for the higher energies. The most neutron-deficient isotope we have studied is ^{101}Sn, in which case the experimental ^{50}Cr(^{58}Ni, $\alpha 3n$) σ value of 16±4 nb represents a fraction of only 1.6×10^{-8} of the total fusion-evaporation cross-section predicted by HIVAP. In this case the predictions from both codes are far from the experimental results and also the predicted energy dependences are different. Both BUSCO and HIVAP overestimate the emission of a ^{12}C cluster and of 3 α particles, respectively. For the ^{58}Ni+^{50}Cr reaction the agreement between experimental data and HIVAP predictions is acceptable only for ^{102}In and to some extent for ^{100}In, whereas for ^{99}Cd and ^{101}Sn the code fails to reproduce the data.

All in all, the calculations yield better agreement with the experimental data for large production cross-sections than for smaller ones. The common feature of the two codes is to predict the σ values for the weak reaction channels to be higher than the measured ones. This may be, for example, related to the fact that shell effects are not completely washed out and thus play a non-negligible role at the excitation energies of the compound nuclei, which are about 50 MeV. Furthermore, the statistical model calculation for low-σ channels, in the last steps of the decay chain, depends very strongly on the level density at very low excitation energies (~8 MeV or less) and thereby the use of a constant level density parameter for all the de-excitation process might be not adequate.

5 Summary and conclusions

We measured the cross sections for ^{99}Cd, ^{100}In, ^{101}Sn and ^{102}In produced as evaporation residues in the reactions ^{58}Ni+^{50}Cr and ^{58}Ni+^{58}Ni, i. e. after light-particle evaporation from ^{108}Te and after cluster emission from ^{116}Ba, respectively. The results indicate that the two reaction mechanisms yield about the same experimental σ for such nuclei very close to ^{100}Sn. On the one hand, it is easy to imagine technical modifications of the on-line separation method, aimed to reduce the losses due to the larger recoil-cone opening for the cluster-accompanied reactions, such as increasing the ion-source entrance window and/or reducing the distance between the ion-source and the target. Such efforts would, of course, only be worth doing if cluster-emission reactions offered *higher* cross sections in producing a given isotope than reactions accompanied by light-particle evaporation. However, the data obtained in this work do

not indicate such an effect. On the other hand, in-beam spectroscopy experiments (2) have evinced that cluster decay has the advantage of yielding higher production cross-sections than light-particle emission. However, this was only achieved for nuclei lying closer to the β-stability valley than those investigated in this work. In this respect cluster decay is an interesting "tool" for producing moderately neutron-deficient isotopes, especially if combined with a recoil mass separator (recoil-tagging technique).

The comparison of the experimental data with statistical-model predictions shows good agreement for isotopes produced with larger cross sections. With the increasing distance of the residues from the valley of β stability the predictions overestimate the data. To improve this situation the following further investigations are to be performed. From the experimental side, measurements of the branching ratios for the βp decay of ^{101}Sn and of ^{100}In are necessary in order to deduce absolute experimental σ values. From the theoretical side more refined calculations are needed, in particular concerning evaporations through weak decay channels that are very interesting for the applications in nuclear-structure studies at the limits of the β–stability valley.

Acknowledgements

The authors would like to thank K. Burkard and W. Hüller for their very competent technical support, and Dr. O. Klepper for the careful collection of very useful information about former measurements done at the GSI on-line mass separator. This work was supported in part by the European Community under Contract No. ERBFMGECT950083. Research at the Oak Ridge National Laboratory is supported by the U.S. Department of Energy under Contract No. DE-AC05-960R22464 with Lockheed Martin Energy Research Corporation.

References

[1] H. Schatz, A. Aprahamian, J. Görres, M. Wiescher, T. Rauscher, J. F. Rembges, F.-K. Thielemann, B. Pfeiffer, P. Möller, K.-L. Kratz, H. Herndl, B. A. Brown, H. Rebel, *Phys. Rep.* **294** (1998) 167.

[2] J. Gómez del Campo, C. Baktash, H.-Q. Jin, D. Rudolph, A. D'Onofrio, F. Terrasi, G. de Angelis, M. De Poli, C. Fahlander, A. Gadea, D. R. Napoli, Q. Pan, P. Spolaore, L. De Acuna, D. Bazzacco, S. Lunardi, P. Pavan, C. Rossi-Alvarez, A. Buscemi, R. Zanon, A. De Rosa, L. Campajola, M. La Commara, G. Inglima, V. Roca, M. Romano, M. Sandoli, M. Romoli, A. Ordine and D. Pierroutsakou, *Phys. Rev.* **C 57** (1998) 2.

[3] Z. Janas, H. Keller, R. Kirchner, O. Klepper, A. Piechaczek, E. Roeckl, K. Schmidt, M. Huyse, J. von Schwarzenberg, J. Szerypo, P. van Duppen, L. Vermeeren, F. Albus, H.-J. Kluge, G. Passler, F. P. Scheerer, N. Trautmann, V. N. Fedoseyev, V. I. Mishin, R. Grzywacz, A. Płochocki, K. Rykaczewski and J. Żylicz, *Phys. Scripta* **56** (1995) 262.

[4] K. Burkard, R. Collatz, M. Hellström, Z. Hu, W. Hüller, O. Klepper, R. Kirchner, E. Roeckl, K. Schmidt, M. Shibata, A. Weber, *Nucl. Inst. and Meth.* **B 126** (1997) 12.

[5] R. Kirchner, K. H. Burkard, W. Hüller, and O. Klepper, *Nucl. Inst. and Meth.* **186** (1981) 295.

[6] J. Szerypo, M. Huyse, G. Reusen, P. van Duppen, Z. Janas, H. Keller, R. Kirchner, O. Klepper, A. Piechaczek, E. Roeckl, D. Schardt, K. Schmidt, R. Grzywacz, M. Pfützner, A. Płochocki, K. Rykaczewski, J. Žylicz, G. Alkhazov, L. Batist, A. Bykov, V. Wittmann, B. A. Brown, *Nucl. Phys.* **A 584** (1995) 221.

[7] T. Elmroth, E. Hagberg, P. G. Hansen, J. C. Hardy, B. Jonson, H. L. Ravn, P. Tidemand-Petersson and the ISOLDE Collaboration, *Nucl. Phys.* **A 304** (1978) 493.

[8] M. Lipoglavšek, J. Cederkäll, M. Palacz, J. Persson, A. Atac, J. Blomqvist, C. Fahlander, H. Grawe, A. Johnson, A. Kerek, W. Klamra, J. Kownacki, A. Likar, L.-O. Norlin, J. Nyberg, R. Schubart, D. Seweryniak, G. de Angelis, P. Bednarczyk, Zs. Dombrádi, D. Foltescu, D. Jerrestam, S. Juutinen, E. Mäkelä, G. Perez, M. De Poli, H. A. Roth, T. Shizuma, Ö. Skeppstedt, G. Sletten, S. Törmänen, T. Vass, *Phys. Rev. Lett.* **76** (1996) 888.

[9] J. Gómez del Campo, R. L. Auble, J. R. Beene, M. L. Halbert, H. J. Kim, A. D'Onofrio, J. L. Charvet, *Phys. Rev.* **C 43** (1991) 2689.

[10] W. Reisdorf, *Z. Phys.* **A 300** (1981) 227 and GSI Report 81-2 (1981) p. 73.

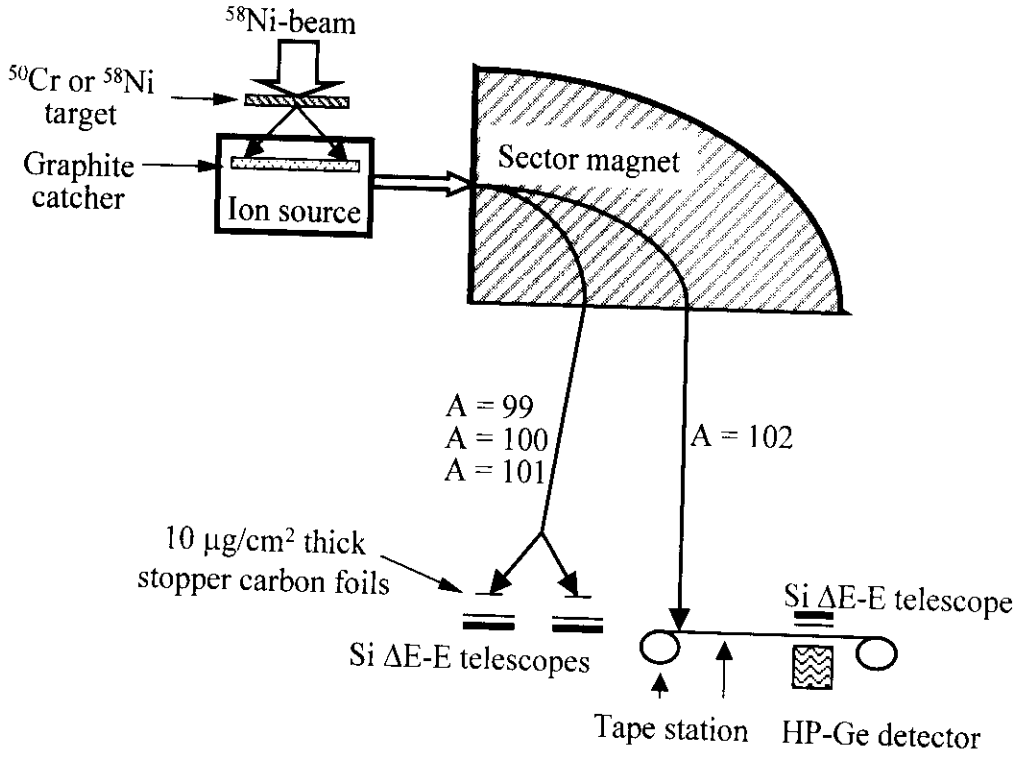

Fig. 1. Outline of the experimental set-up (see text for details).

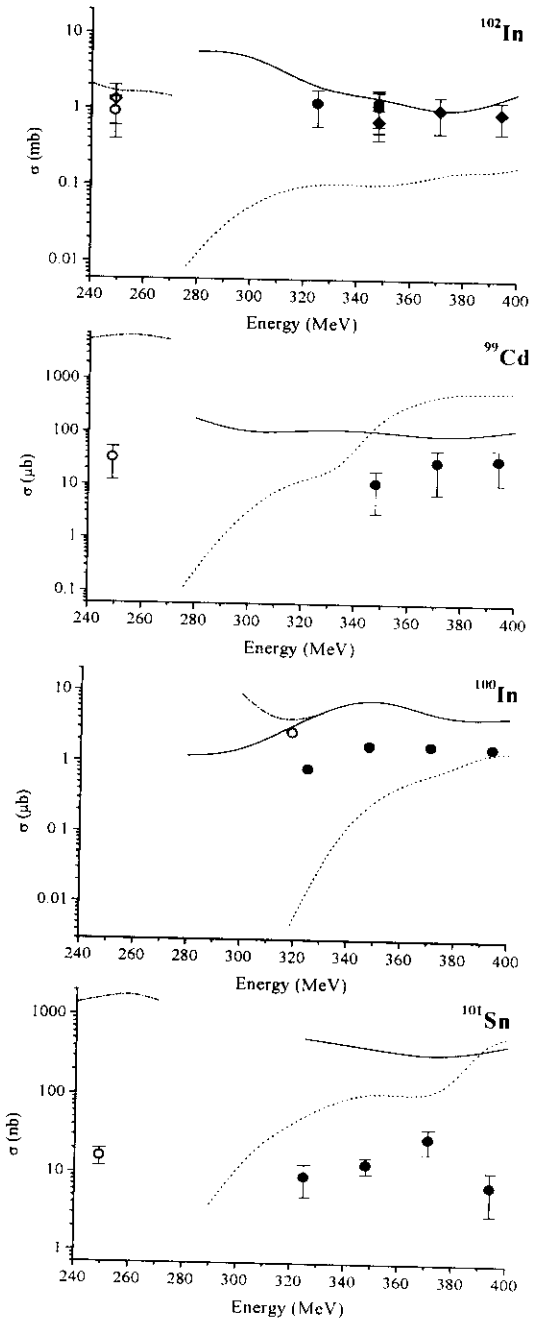

Fig. 2. Experimental and calculated σ values as a function of the ^{58}Ni-beam energy in the middle of targets. The data for the ^{58}Ni+^{50}Cr reaction (open circles) and the ^{58}Ni+^{58}Ni one (solid circles) were deduced from βp activities; for ^{102}In further data were deduced from $\beta\gamma$ activity for the ^{58}Ni+^{50}Cr reaction (open diamonds) and for the ^{58}Ni+^{58}Ni one (solid diamonds). The data for ^{100}In represent upper limits. The calculations represent HIVAP predictions for the ^{58}Ni+^{50}Cr reaction (dash-dotted line) and for the ^{58}Ni+^{58}Ni one (dotted line), and BUSCO predictions for ^{58}Ni+^{58}Ni reaction (solid line).

Table 1
Compilation of the experimental cross sections σ. The values marked by an asterisk were deduced from ^{102}In $\beta\gamma$ activity, whereas those marked by a diamond or a double diamond correspond, to results from a former in-beam measurement and from a previous on-line mass separation experiment, respectively. All other σ values stem from βp measurements. The evaporation channels are inferred from statistical-model calculation results.

Reaction	Beam energy# (MeV)	Evaporation channel	Residual nucleus	σ (mbarn)
^{58}Ni+^{50}Cr	249	αpn	^{102}In	0.9±0.5
^{58}Ni+^{50}Cr	249	αpn	^{102}In	1.3±0.7*
^{58}Ni+^{50}Cr	348	αpn	^{102}In	1.1±0.6
^{58}Ni+^{58}Ni	325	^{12}Cpn	^{102}In	1.2±0.6
^{58}Ni+^{58}Ni	348	^{12}Cpn	^{102}In	1.2±0.6
^{58}Ni+^{58}Ni	348	^{12}Cpn	^{102}In	0.7±0.3*
^{58}Ni+^{58}Ni	371	^{12}Cpn	^{102}In	1.0±0.5*
^{58}Ni+^{58}Ni	394	^{12}Cpn	^{102}In	0.9±0.4*
^{58}Ni+^{50}Cr	249	$2\alpha n$	^{99}Cd	(3.2±2.0) $\times10^{-2}$
^{50}Cr+^{58}Ni	225	$2\alpha n$	^{99}Cd	(2.5±0.8) $\times10^{-2}$ ◇
^{58}Ni+^{58}Ni	348	^{12}Cαn	^{99}Cd	(1.1±0.8) $\times10^{-2}$
^{58}Ni+^{58}Ni	371	^{12}Cαn	^{99}Cd	(2.8±2.1) $\times10^{-2}$
^{58}Ni+^{58}Ni	394	^{12}Cαn	^{99}Cd	(3.1±2.0) $\times10^{-2}$
^{58}Ni+^{50}Cr	319	$\alpha p3n$	^{100}In	2.6 $\times10^{-3}$
^{58}Ni+^{58}Ni	325	^{12}C$p3n$	^{100}In	0.8 $\times10^{-3}$
^{58}Ni+^{58}Ni	348	^{12}C$p3n$	^{100}In	1.7 $\times10^{-3}$
^{58}Ni+^{58}Ni	371	^{12}C$p3n$	^{100}In	1.7 $\times10^{-3}$
^{58}Ni+^{58}Ni	394	^{12}C$p3n$	^{100}In	1.6 $\times10^{-3}$
^{58}Ni+^{50}Cr	249	$\alpha 3n$	^{101}Sn	(1.6±0.4) $\times10^{-5}$
^{58}Ni+^{50}Cr	250	$\alpha 3n$	^{101}Sn	(1.0) $\times10^{-5}$ ◇◇
^{58}Ni+^{58}Ni	325	^{12}C$3n$	^{101}Sn	(0.9±0.4) $\times10^{-5}$
^{58}Ni+^{58}Ni	348	^{12}C$3n$	^{101}Sn	(1.3±0.3) $\times10^{-5}$
^{58}Ni+^{58}Ni	371	^{12}C$3n$	^{101}Sn	(2.8±1.0) $\times10^{-5}$
^{58}Ni+^{58}Ni	394	^{12}C$3n$	^{101}Sn	(0.7±0.4) $\times10^{-5}$

Calculated by taking the ^{58}Ni-beam energy loss in half of the target thickness into account.